Color and luminance information in natural scenes

C. A. Párraga, G. Brelstaff,* and T. Troscianko

Perceptual Systems Research Centre, Department of Psychology, 8 Woodland Road, University of Bristol, BS8 1TN, UK

I. R. Moorehead

WX1 Department, Defence Evaluation and Research Agency, Fort Halstead, Sevenoaks, Kent 14 7BP, UK

Received October 11, 1996; revised manuscript received March 10, 1997; accepted April 16, 1997

The spatial filtering applied by the human visual system appears to be low pass for chromatic stimuli and band pass for luminance stimuli. Here we explore whether this observed difference in contrast sensitivity reflects a real difference in the components of chrominance and luminance in natural scenes. For this purpose a digital set of 29 hyperspectral images of natural scenes was acquired and its spatial frequency content analyzed in terms of chrominance and luminance defined according to existing models of the human cone responses and visual signal processing. The statistical $1/f$ amplitude spatial-frequency distribution is confirmed for a variety of chromatic conditions across the visible spectrum. Our analysis suggests that natural scenes are relatively rich in high-spatial-frequency chrominance information that does not appear to be transmitted by the human visual system. This result is unlikely to have arisen from errors in the original measurements. Several reasons may combine to explain a failure to transmit high-spatial-frequency chrominance: (a) its minor importance for primate visual tasks, (b) its removal by filtering applied to compensate for chromatic aberration of the eye's optics, and (c) a biological bottleneck blocking its transmission. In addition, we graphically compare the ratios of luminance to chrominance measured by our hyperspectral camera and those measured psychophysically over an equivalent spatial-frequency range. [S0740-3232(98)00303-2]

OCIS codes: 330.1690, 330.6110, 260.3800.

1. INTRODUCTION

A. Context

A series of studies of how the human visual system (HVS) encodes and transmits retinal imagery has increasingly advocated a role for natural scenes as a formative force. In this approach, evolutionary pressure may provide the impetus for the HVS to adopt efficient visual representations in an information-theoretic sense.[1–3] By coding first the things that matter most (food, predators, mates, etc.) the fittest visual system ought to survive. In this scenario, the statistical spatiochromatic properties of natural scenes help mold the spatiochromatic characteristics of the early visual pathways so that they reduce redundancy and separate essential signal from noise. This approach has been successfully used by Atick[3] to predict the physiologically measured responses of certain cells in lateral geniculate nucleus (LGN). The assumptions underlying this prediction include a constraint on the spatial frequency (SF) makeup of natural scenes over a range of chromatic conditions. This constraint, commonly termed the $1/f$ law, requires that the average Fourier amplitude of natural images fall off inversely with SF. Measurement has shown this to be roughly true for achromatic images.[4,5] However, as yet, the evidence that $1/f$ applies in a variety of chromatic conditions has been at best inconclusive.[6–8] We present here new measurements that further confirm the $1/f$ assumption over a wider variety of chromatic conditions.

Note that a $1/f$ law does not imply that the luminance contrast sensitivity function (CSF) should simply match $1/f$, because as is implied by Atick such a CSF would transmit a lot of noise. By explicitly modeling an early noise-suppression stage he shows how a recognizable luminance CSF can be predicted.

Atick investigated only linear transformations as candidate coding schemes. Basically, this means that his LGN cells simply compute weighted sums or differences of their inputs: in our terms these may represent luminance or chrominance (e.g., L + M or L − M, respectively, where L derives from the red cones and M from the green). As recent developments in artificial neural networks[9] and single-cell recording[10] techniques reveal, single cells might be computing sophisticated nonlinear functions of their inputs. With this in mind, we present results for a simple nonlinear (divisive) transformation in addition to some previously established linear transformations. In the absence of other guidance, our nonlinear transformation is motivated by the desire to represent colored objects in a way that is independent of the shadowing that pervades natural scenes. In particular, we have investigated the definitions of luminance = L + M and chrominance = (L − M)/(L + M).

This formulation has the advantage of retaining the L − M subtractive element to chrominance while ensuring that a cast-shadow boundary that typically attenuates L and M by similar amounts effects a luminance step but produces little or no change in chrominance. We precede

details of our investigation by a review of some evidence and models underpinning it.

B. Evidence

Both physiological and psychological evidence suggests that the HVS analyzes images by employing neural subsystems tuned to different attributes of the stimulus (color, texture, and movement) that vary in their degrees of spatial and temporal resolution. In particular, the psychophysically measured CSF's for visual stimuli modulated in luminance and chrominance show different profiles.

Chrominance modulation (of red–green isoluminant color design) is not seen at high SF above ~12 cycles/deg, whereas luminance modulation has been reported to be visible up to[11] and beyond[12] 30 cycles/deg. Furthermore, luminance sensitivity appears to peak near 2 cycles/deg and drops off at lower SF's (thus achieving band-pass filtering), whereas sensitivity to isoluminant color is highest at those low SF's (and is low-pass filtered). We restrict our consideration to red–green opponent definitions and do not address the blue–yellow system, with its complication of sparser retinal coverage, nor peripheral vision.

A qualitative division into band-pass luminance and low-pass chrominance transmission prevails also in physiological measurements[13,14] of the single cells in parvocellular layers of LGN in macaque (with much similarity to the HVS). The responses measured to modulations in luminance or chrominance show that the majority of cells (coined "Type-I R–G") exhibit center-surround receptive fields that simultaneously encode band-pass luminance and low-pass chrominance signals. It is not clear precisely how the signals from these cells might propagate to generate psychophysically measured sensation, nor whether other visual pathways might be involved to significant extents.[15] However, it is interesting to note that these Type-I R–G cells, considered leading candidates for the early transmission of chromatic and luminance information, do seem to share similar SF characteristics as the final output (single cells, however, have narrower bandwidths).

C. Multiplex Model

A multiplex model[16,17] (analogous to that of AM radio transmission) may be used to picture the SF banding in the signal transmitted from a single Type-I R–G cell. Demultiplexing this signal after transmission to striate cortex might provide components of luminance and chrominance from which the psychophysical CSF's could be derived. Summing the signals transmitted by opposite pairs of co-located opponent cells (i.e., a red-center/green-surround and a green-center/red-surround) could fully recover both components.[18] However, this would require two neurons transmitting down the optic nerve instead of one, and so some alternatives have been considered. Demultiplexing the signal from a single neuron into two discrete SF bands can only partially recover the original components: because their SF domains do overlap, the reconstructed chrominance would be contaminated by any low-SF luminance modulations, and reconstructed luminance would contain any high-SF chrominance modulation. In either case the degree of cross talk (contamination) depends on the SF content of the signals actually carried.

A large amount of cross talk might normally be expected in low-SF chrominance because low-SF luminance stimuli are abundant in natural scenes. A single cell that is operating noise supression according to Atick's model should theoretically transmit less low-SF luminance and thus cause less cross talk. Conversely, the amount of cross talk in the luminance signal will depend on the quantity of high-SF chromatic signal arriving at the Type-I R–G cell. This in turn will depend on the relative abundance of high-SF chrominance in natural scenes, as well as on the optical and retinal factors.

As a provisional quantification of the cross-talk problem that might be faced by the HVS, we describe below an analysis of our hyperspectral measurements in terms of the ratio of the Fourier amplitudes of luminance to those of chrominance, across SF, for various definitions.

Bear in mind that—since we have not explicitly modeled noise suppression—the ratios may be biased and difficult to interpret. Further, note that our measuring device precludes analysis of ratios nominally beyond 9 cycles/deg.

D. Definitions

Previous studies have motivated various definitions of luminance and chrominance in terms of the Smith–Pokorny cone responses.[19,20] We adopt three linear definitions from the literature and add our own nonlinear definition. In our case only the L- and M-cone responses are involved, and our computations assume that their spectral curves or normalized so as to peak at unity. The definitions are as follows:

(a) Simple definition:

$$\mathrm{lum}_s = \mathrm{L} + \mathrm{M},$$
$$\mathrm{chrom}_s = \mathrm{L} - \mathrm{M}.$$

(b) Ingling–Tsou[21] definition, motivated by flicker and acuity criteria:

$$\mathrm{lum}_{\mathrm{IT}} = 1.02\mathrm{L} + \mathrm{M},$$
$$\mathrm{chrom}_{\mathrm{IT}} = 0.41\mathrm{L} - \mathrm{M}.$$

(c) Buchsbaum–Gottschalk[22] definition, derived from a principal-components analysis of the cone responses:

$$\mathrm{lum}_{\mathrm{BG}} = 0.887\mathrm{L} + 0.461\mathrm{M},$$
$$\mathrm{chrom}_{\mathrm{BG}} = 0.46\mathrm{L} - 0.88\mathrm{M}.$$

(d) Shadow-removing definition:

$$\mathrm{lum}_{\mathrm{sr}} = \mathrm{L} + \mathrm{M},$$
$$\mathrm{chrom}_{\mathrm{sr}} = \frac{\mathrm{L} - \mathrm{M}}{\mathrm{L} + \mathrm{M}} = \frac{\mathrm{chrom}_s}{\mathrm{lum}_s}.$$

In practice, our hyperspectral measurements for each scene allow values of L and M to be computed from 31 narrow-band radiance images. The data set of all 29 scenes is being made available to other re-searchers at an ftp site posted at http://www.crs4.it/~gjb/ftpJOSA.html. In the UK it is http://www.mrc-bbc.ox.ac.uk/~rjb/COLOUR/ftp JOSA.html.

2. METHODS

A. Hyperspectral Camera

The hyperspectral camera, further described elsewhere,[23] measures radiance as a function of wavelength for each image pixel. It consists of an electro-optic mechanism built around a Pasecon integrating camera tube, a camera control unit, a carousel slide-changing filter mechanism, a portable PC, a video monitor, and a battery power supply. The Pasecon has good linearity throughout the visible spectrum and is able to integrate signal over a computer-selected interval, thus permitting a reasonable signal-to-noise ratio even at the low light levels incurred by using narrow-band filters. A light-tight, slide-changing filter mechanism allows the camera to acquire images sequentially through the set of 31 optical interference filters that span the range 400–700 nm and with nominal 10-nm spacing. The entire system is controlled by the PC and mounted on a trolley along with a power supply kit. A manual, fixed-focal-length lens (Fuji CF25B, $f/1.4$, 25 mm) with a field angle of 28.71 h deg × 21.73 v deg is employed. An MS-DOS C program sends a value for the integration time to the camera control unit, which digitizes each image and transfers it to the PC frame card. The whole system acquires a sequence of 31 chromatically narrow-band-filtered 8-bit, 256 × 256 pixel images in less than 5 min.

Concerning the modulation transfer function of the system, there are two possible issues: (a) the possibility of aliasing of spatial frequencies above the Nyquist limit (9.0 cycles/deg) and (b) effects of wavelength (e.g., those due to chromatic aberration of the camera lens). For (a), tests were performed on synthetic scenes that showed no intrusion of aliasing of higher SF's in the Fourier spectra of the images in the range used in this study; for (b), there was no effect of wavelength in the relevant range. There was a small reduction in modulation for high SF's below 450 nm, but these wavelengths do not provide a significant input to the L- and M-cone primaries.

Individual interference filters differ in their degree of flatness and thus may systematically displace their images slightly on the camera target. These shifts (no more than 2 pixels) once calibrated are routinely corrected on the frame card. Each image corresponds only to the central part of the visual field supplied by the lens. The field angle is equal to 14.35 deg × 14.35 deg, and each pixel subtends an angle of approximately 0.056 deg × 0.56 deg (3.36 arc min)—which is not quite the same order of the size as a foveal cone (~0.5 arc min). Once recorded, the image set is archived on a UNIX workstation, where measured radiance is computed for each interference filter with use of a different conversion function. Each function depends on the pixel gray level, pixel position, filter transmission, lens f-stop, and tube integration time. The calibration function was determined in the dark room. The calibration process involved a Kodak standard gray card, a TopCon SR1 spectrometer, and a target collage of colored papers under illumination by a steady-current light source. The relative error of the camera compared with the SR1 was less than 5% in the range 400–570 nm and 10% in the range 580–700 nm. The worst case (20% relative error) was found for one red test patch in the extreme red[23] (650–700 nm).

Given the long acquisition time, scenes were recorded under stable weather and lighting conditions. Outdoor scenes were recorded around noon to minimize changes of illumination, and sometimes it was necessary to wait until the sky was completely clear or completely overcast before starting. Unfortunately this greatly restricts the quantity of cast shadows in our data. Some scenes were recorded inside the glass houses of the Bristol Botanical Gardens to avoid small movements of branches and leaves occasioned by the wind, and out of doors some objects at short distance were avoided.

B. Characteristics of the Data Set

Although there is no formal agreement about what is considered a representative sampling of the visual environment, we hoped to ensure that some of the most common natural objects were represented in our data set. These include plants with different shapes, textures and colors, flowers (often bright red), trunks, branches, grass, green and yellow leaves, trees, bushes, rocks, and sky. Figure 1 shows four achromatic representations of images used for this study. Many scenes are of the English countryside and gardens—in which buildings or other human artifacts are avoided. Others are of natural objects arranged in the laboratory to look fairly naturalistic. Our general aim was to acquire a set of scenes that could conceivably be representative of the environment in which primate vision evolved. Of course, we cannot be sure that we have achieved this aim. However, the inclusion of vegetation seen from different distances goes some way toward satisfying this requirement.

Several practical constraints also limited our choices. Bright sky and reflecting water result in large saturated areas of the image and are deliberately avoided. Only four of our scenes contain regions of sky. Drifting objects

Fig. 1. Example of typical images from our data set.

Table 1. Range and Central Spatial Frequency (in Cycles/Deg) of SF Bands Used to Divide the Fourier Space

Band	Range (cycles/deg)	Central SF (cycles/deg)
1	0.03–0.07	0.05
2	0.07–0.14	0.10
3	0.14–0.28	0.21
4	0.28–0.55	0.41
5	0.55–1.10	0.83
6	1.10–2.20	1.65
7	2.20–4.40	3.30
8	4.40–8.80	6.60

such as clouds and strong shadows are also avoided. All scenes were recorded between October 1993 and January 1994.

C. Image Processing

A standard two-dimensional fast-Fourier-transform algorithm was available to derive for a given scene the Fourier amplitude spectrum either of each individual narrow-band-radiance image or of combinations of the images, in all forms of lum and chrom images as defined previously. From all such images it was then possible to measure the total amplitude contained within a set of chosen SF bands. These bands, labeled 1–8 in Table 1, are centered at equal intervals on a logarithmic scale and do not overlap. Band 1 omits the zeroth SF so to exclude the direct influence of a scene's illumination level. To favor equality in the subsequent statistical representation of scenes, all lum and chrom images are individually normalized to contain unit total Fourier amplitude. We do not mean, however, to imply that chrominance is *a priori* of the same importance as luminance: the normalization is merely a graphical convenience and does not unduly affect our conclusions.

3. RESULTS

A. Measurements of 1/*f*

The results summarized in Fig. 2 demonstrate that the $1/f$ law approximately holds even for 10-nm chromatic bands. Expressing the Fourier amplitude distribution of spectral radiance as f^{α} allows a measurement of the slope α, which should be -1 if $1/f$ holds. The value of α, plotted for each 10-nm interval, results from fitting a straight line to the SF distribution of the mean Fourier amplitude. In particular, the SF distribution is sampled at the center of each of the eight bands in Table 1, and the mean amplitude is computed from all 29 scenes. In this case, each scene is given equal statistical weight by first normalizing its total SF amplitude across all wavelengths to be unity (again ignoring the zeroth SF). As the plot shows, slope α varies between approximately -1.08 and -1.16. This result is very similar to that previously reported by the authors for derived reflectance.[23]

As might be expected, computed luminance and chrominance also roughly obey $1/f$. Figure 3 gives an idea of the variability encountered between scenes. It plots amplitude spectra in lum for four example images of the data set. Figure 4 plots the mean amplitude over all 29 scenes in lum and chrom, each exhibiting $1/f$-like behavior. In this case the simple definition of chrom is used. Figure 5 plots the same for the shadow-removing definition, with similar results. Table 2 quantifies the mean values of the slope α for both definitions.

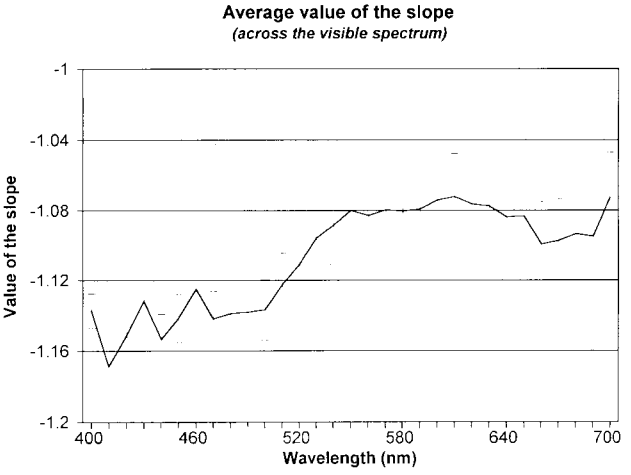

Fig. 2. Mean value of the slope (α) across wavelength. Scenes were converted into radiance, and their Fourier amplitude spectra were normalized to 1. Standard error is shown in the plot.

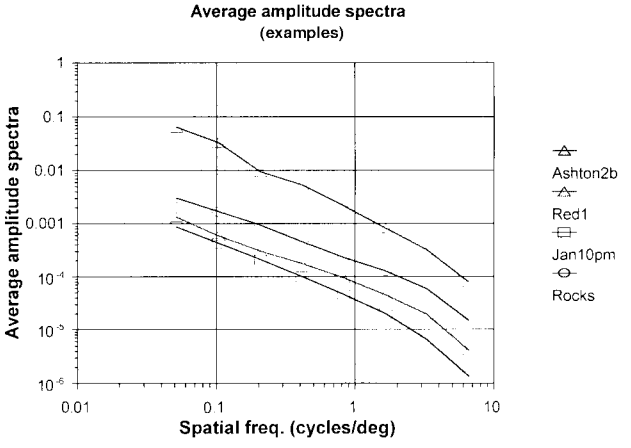

Fig. 3. Amplitude spectrum (lum) for some scenes of our data set (simple definition).

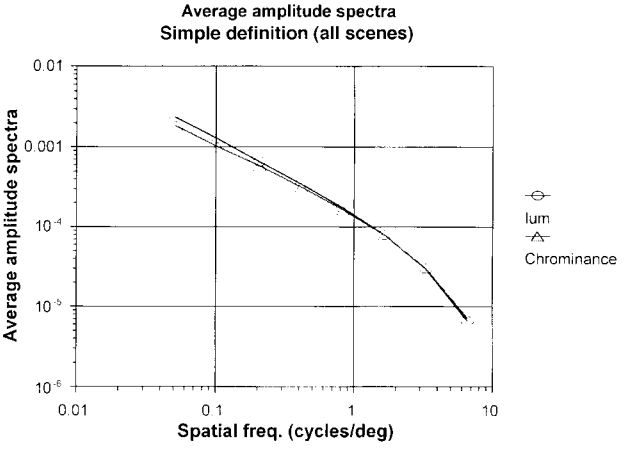

Fig. 4. Amplitude spectrum for lum and chrom for all of the data set (29 scenes) (simple definition).

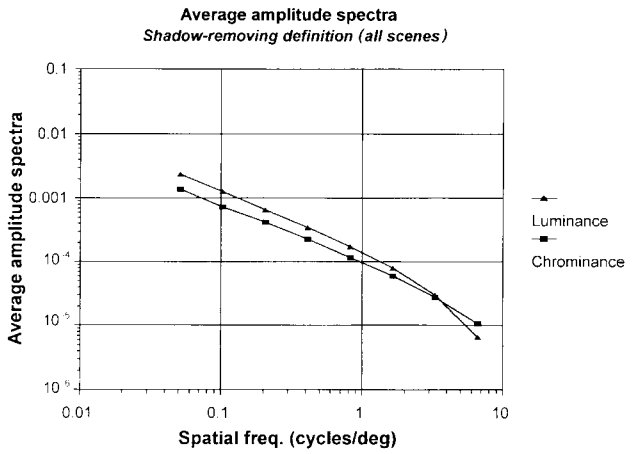

Fig. 5. Amplitude spectrum for lum and chrom for all of the data set (29 scenes) (shadow removing).

Table 2. Mean Values of the Slope (α) for the Simple and the Shadow-Removing Definitions of Lum and Chrom

Slope (α)	Simple Definition	Shadow-Removing Definition
Lum	-1.11 ± 0.13	-1.11 ± 0.13
Chrom	-1.06 ± 0.11	-0.94 ± 0.12

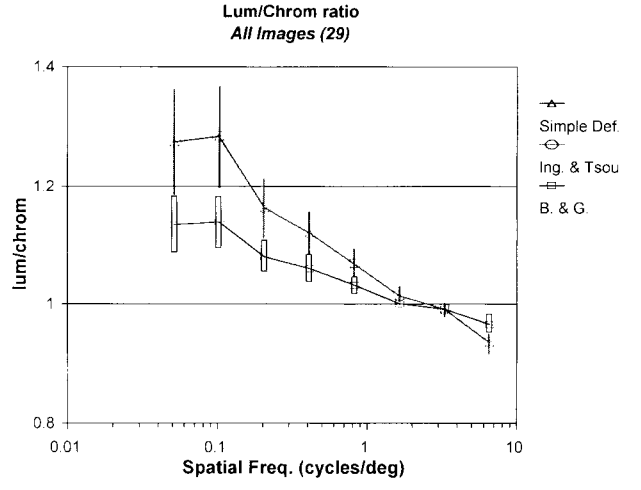

Fig. 6. Mean ratio of the lum image to that of the chrom image amplitude for all of the data set. The three definitions are used. Standard error is shown on the plot.

Any discrepancy from $1/f$ occurs at high SF and could possibly be artifacts of our imaging system, such as fine-scale variations during acquisition perhaps due to wind effects. These effects would have been expected to be most profound in short-distance outdoor scenes and thus motivated our analysis of bias described below.

B. Measurements of the Lum/Chrom Ratio

The ratio of the lum image amplitude to that of the chrom image amplitude is plotted for each SF band. Figure 6 shows the mean across all scenes of this ratio for all three linear definitions. In the case of the simple and the Ingling–Tsou definitions the results are coincident. For low SF there is relatively more luminance than chrominance. This is reversed only for the highest SF considered in the plot (the value of lum/chrom is lower than 1).

The Buchsbaum–Gottschalk definition, while not coincident, produces a similar trend. Figure 7 shows the results for the divisive shadow-removing definition. The basic features are the same. The only notable new feature is the change in the shape of the plot. One explanation for the similarity could be the avoidance of sharp shadows in our data set.

C. Analysis of the Bias of the Data Set

Figure 8 was produced by analyzing two sets of scenes separately. The first set (called short-distance viewing set) consists of scenes in which the objects were up to 10 m away from the camera. The second set (called long-distance viewing set) consists of scenes in which most of the objects (e.g., trees) were farther than 10 m away. The plot suggests that the statistics of this long-distance viewing set of scenes may be different from the others. This biasing might be due to the considerable proportion (~50%) of grass and sky in the scene.

We attempted other classifications of the scenes of our data set in order to check whether the quality of the pictures or the lighting (artificial or natural) might influence our results. None of these proved to determine the appearance our plots. We chose a best-quality set of ten scenes to evaluate the presence of artifacts in our data set. Figure 9 shows the results of averaging over short-distance viewing scenes. The data set is divided into artificially lit (indoor) scenes, naturally lit (outdoor) scenes, and best-quality scenes. However, there seems to be little difference among these potentially different types of scene.

4. DISCUSSION

Regarding the whole of the HVS simply as a black box, whose CSF's may be revealed by psychophysical experiment, leads to the inevitable view that the CSF's mismatch the SF content of natural scenes. Our results

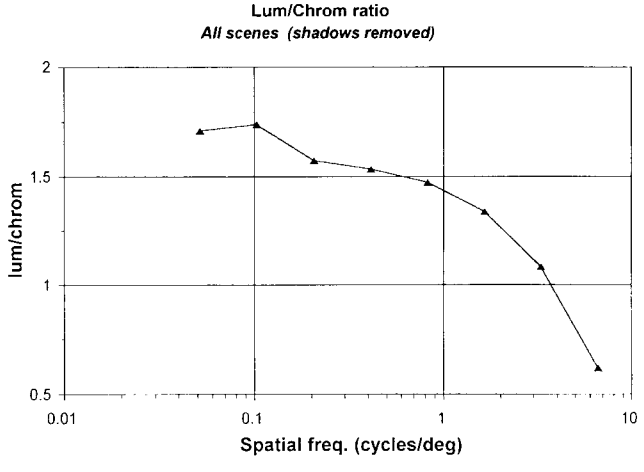

Fig. 7. Mean ratio of the lum image amplitude to that of the chrom image amplitude with the shadow-removing definition of lum and chrom. This average is done across all of the data set.

however, our data set is focused most sharply around the peaks of the L and M cones; and Mullen[11] took considerable care to keep chromatic aberration from influencing her CSF's. So, although we have no concrete support, it is possible that the HVS discards high-SF color because it forms part of the message that carries aberrated data about the real world.[26]

3. Physiological constraints: The optic nerve is a bottleneck in the information path from the retina to subsequent brain centers; there are insufficient neurons to transmit the retinal information. There is therefore strong pressure to maximize the amount of information transmitted per optic nerve neurons, which implies strong postreceptoral recoding of the stimulus information designed to maximize the efficiency of this information transmission. As discussed in Section 1, this kind of data compression might have to be lossy and the HVS may have evolved to lose high-SF color, and this might be achieved by some sort of multiplexing technique.

5. CONCLUSIONS

A new hyperspectral data set of 29 natural scenes was acquired and made available for spatiochromatic analysis. Our preliminary analysis of the ratio of luminance to chrominance Fourier amplitudes in these scenes suggests a mismatch between spatial-frequency content of the natural world and the human visual system's contrast-sensitivity functions. The mismatch might be due to quantum-noise suppression, as discussed by Atick.[3] The $1/f$ law that Atick's analysis assumes has been confirmed to approximately hold for both narrow- and broad-band chromatic spectra. We have discussed the following possible reasons as to why the HVS appears to discard high-SF chrominance: (1) its irrelevance to primate vision, (2) its removal by neural machinery that may compensate for chromatic aberrations, and (3) lossy data compression in response to physiological constraints.

ACKNOWLEDGMENTS

The construction of the hyperspectral camera was supported by a grant from the UK Defence Research Agency under grant D/ER1/9/4/2034/102/RARDE. We thank Derek Carr for technical support and Kay Nelson and Julian Partridge for help with image acquisition. Comments from two anonymous reviewers have been particularly helpful. The shadow-removing definition of chrominance benefited from discussion with Fred Kingdom.

*Now with CRS4, via N. Sauro 10, Cagliari, 09123, Italy.

REFERENCES

1. H. B. Barlow, "Possible principles underlying the transformation of sensory messages," in *Sensory Communications*, W. A. Rosenblith, ed. (MIT Press, Cambridge, Mass., 1961), pp. 217–234.
2. M. V. Srinivasan, S. B. Laughlin, and A. Dubs, "Predicitive coding: a fresh view of inhibition in the retina," Proc. R. Soc. London, Ser. B **216**, 427–459 (1982).
3. J. J. Atick, "Could information theory provide an ecological theory for sensory processing?" Network **3**, 231–251 (1992).
4. D. J. Field, "Relation between the statistics of natural scenes and the response properties of cortical cells," J. Opt. Soc. Am. A **4**, 2379–2394 (1987).
5. D. J. Tolhurst, Y. Tadmor, and Tang Chao, "Amplitude spectra of natural images," Ophthalmic. Physiol. Opt. **12**, 229–232 (1992).
6. G. J. Burton and I. R. Moorhead, "Color and spatial structure in natural scenes," Appl. Opt. **26**, 157–170 (1987).
7. G. Brelstaff and T. Troscianko, "Information content of natural scenes: implications for neural coding of color and luminance," in *Human Visual Processing and Digital Display*, B. E. Rogowitz, ed., Proc. SPIE **1666**, 302–309 (1992).
8. J. B. Derrico and G. Buchsbaum, "A computational model of spatiochromatic image coding in early vision," J. Visual Commun. Image Represent. **2**, 31–37 (1991).
9. S. M. Courtney, L. H. Finkel, and G. Buchsbaum, "A multistage neural network for colour constancy and color induction," IEEE Trans. Neural Netw. **6**, 972–985 (1995).
10. C. Koch, "Computation and the single neuron," Nature **385**, 207–210 (1997).
11. K. T. Mullen, "Contrast sensitivity of human color vision to red–green and blue–yellow chromatic gratings," J. Physiol. (London) **359**, 381–400 (1985).
12. R. L. De Valois, H. Morhan, and D. M. Snodderly, "Psychophysical studies of monkey vision III. Spatial luminance contrast sensitivity tests of macaque and human observers," Vision Res. **14**, 75–81 (1974).
13. A. M. Derrington and P. Lennie, "Spatial and temporal contrast sensitivities of neurons in lateral geniculate nucleus of macaque," J. Physiol. (London) **357**, 219–240 (1984).
14. A. M. Derrington, J. Krauskopf, and P. Lennie, "Chromatic mechanisms in lateral geniculate nucleus of macaque," J. Physiol. (London) **357**, 241–265 (1984).
15. R. L. De Valois and K. K. De Valois, "A multi-stage color model," Vision Res. **33**, 1053–1065 (1993).
16. C. R. Ingling, Jr., and E. Martinez, "The spatiochromatic signal of the $r-g$ channel," in *Color Vision: Physiology and Psychophysics*, J. D. Mollon and L. T. Sharpe, eds. (Academic, London, 1983), pp. 433–444.
17. F. A. A. Kingdom and K. T. Mullen, "Separating color and luminance information in the visual system," Spatial Vis. **9**, 191–219 (1995).
18. M. D'Zmura and P. Lennie, "Mechanisms of color constancy," J. Opt. Soc. Am. A **3**, 1662–1672 (1986).
19. C. Smith and J. Pokorny, "Spectral sensitivity of the foveal cone photopigments between 400 and 500 nm," Vision Res. **15**, 161–171 (1975).
20. D. Travis, *Effective Color Displays* (Academic, London, 1991), App. 4, pp. 271–272.
21. C. R. Ingling, Jr., and B. H. Tsou, "Spectral sensitivity for flicker and acuity criteria," J. Opt. Soc. Am. A **5**, 1374–1378 (1988).
22. G. Buchsbaum and A. Gottschalk, "Trichomacy, opponent color coding and optimum color information transmission in the retina," Proc. R. Soc. London, Ser. B **220**, 80–113 (1983).
23. G. Brelstaff, A. Párraga, T. Troscianko, and D. Carr, "Hyperspectral camera system: acquisition and analysis," in *Geographic Information Systems, Photogrammetry, and Geological/Geophysical Remote Sensing*, J. B. Lurie, J. J. Pearson, and E. Zillioli, eds., Proc. SPIE **2587**, 150–159 (1995).
24. J. D. Mollon, "Tho' she kneel'd in that place where they grew.... The uses and origins of primate colour vision," J. Exp. Biol. **146**, 21–38 (1989).
25. Y. Le Grand, *Form and Space Vision* (translated by Michel Millodot and Gordon G. Heat, Indiana U. Press, Bloomington and London, 1967), pp. 5–35.
26. M. V. Berry and A. N. Wilson, "Black and white fringes and the colours of caustics," Appl. Opt. **33**, 4714–4964 (1994).

however, our data set is focused most sharply around the peaks of the L and M cones; and Mullen[11] took considerable care to keep chromatic aberration from influencing her CSF's. So, although we have no concrete support, it is possible that the HVS discards high-SF color because it forms part of the message that carries aberrated data about the real world.[26]

3. Physiological constraints: The optic nerve is a bottleneck in the information path from the retina to subsequent brain centers; there are insufficient neurons to transmit the retinal information. There is therefore strong pressure to maximize the amount of information transmitted per optic nerve neurons, which implies strong postreceptoral recoding of the stimulus information designed to maximize the efficiency of this information transmission. As discussed in Section 1, this kind of data compression might have to be lossy and the HVS may have evolved to lose high-SF color, and this might be achieved by some sort of multiplexing technique.

5. CONCLUSIONS

A new hyperspectral data set of 29 natural scenes was acquired and made available for spatiochromatic analysis. Our preliminary analysis of the ratio of luminance to chrominance Fourier amplitudes in these scenes suggests a mismatch between spatial-frequency content of the natural world and the human visual system's contrast-sensitivity functions. The mismatch might be due to quantum-noise suppression, as discussed by Atick.[3] The $1/f$ law that Atick's analysis assumes has been confirmed to approximately hold for both narrow- and broad-band chromatic spectra. We have discussed the following possible reasons as to why the HVS appears to discard high-SF chrominance: (1) its irrelevance to primate vision, (2) its removal by neural machinery that may compensate for chromatic aberrations, and (3) lossy data compression in response to physiological constraints.

ACKNOWLEDGMENTS

The construction of the hyperspectral camera was supported by a grant from the UK Defence Research Agency under grant D/ER1/9/4/2034/102/RARDE. We thank Derek Carr for technical support and Kay Nelson and Julian Partridge for help with image acquisition. Comments from two anonymous reviewers have been particularly helpful. The shadow-removing definition of chrominance benefited from discussion with Fred Kingdom.

*Now with CRS4, via N. Sauro 10, Cagliari, 09123, Italy.

REFERENCES

1. H. B. Barlow, "Possible principles underlying the transformation of sensory messages," in *Sensory Communications*, W. A. Rosenblith, ed. (MIT Press, Cambridge, Mass., 1961), pp. 217–234.
2. M. V. Srinivasan, S. B. Laughlin, and A. Dubs, "Predicitive coding: a fresh view of inhibition in the retina," Proc. R. Soc. London, Ser. B **216**, 427–459 (1982).
3. J. J. Atick, "Could information theory provide an ecological theory for sensory processing?" Network **3**, 231–251 (1992).
4. D. J. Field, "Relation between the statistics of natural scenes and the response properties of cortical cells," J. Opt. Soc. Am. A **4**, 2379–2394 (1987).
5. D. J. Tolhurst, Y. Tadmor, and Tang Chao, "Amplitude spectra of natural images," Ophthalmic. Physiol. Opt. **12**, 229–232 (1992).
6. G. J. Burton and I. R. Moorhead, "Color and spatial structure in natural scenes," Appl. Opt. **26**, 157–170 (1987).
7. G. Brelstaff and T. Troscianko, "Information content of natural scenes: implications for neural coding of color and luminance," in *Human Visual Processing and Digital Display*, B. E. Rogowitz, ed., Proc. SPIE **1666**, 302–309 (1992).
8. J. B. Derrico and G. Buchsbaum, "A computational model of spatiochromatic image coding in early vision," J. Visual Commun. Image Represent. **2**, 31–37 (1991).
9. S. M. Courtney, L. H. Finkel, and G. Buchsbaum, "A multistage neural network for colour constancy and color induction," IEEE Trans. Neural Netw. **6**, 972–985 (1995).
10. C. Koch, "Computation and the single neuron," Nature **385**, 207–210 (1997).
11. K. T. Mullen, "Contrast sensitivity of human color vision to red-green and blue-yellow chromatic gratings," J. Physiol. (London) **359**, 381–400 (1985).
12. R. L. De Valois, H. Morhan, and D. M. Snodderly, "Psychophysical studies of monkey vision III. Spatial luminance contrast sensitivity tests of macaque and human observers," Vision Res. **14**, 75–81 (1974).
13. A. M. Derrington and P. Lennie, "Spatial and temporal contrast sensitivities of neurons in lateral geniculate nucleus of macaque," J. Physiol. (London) **357**, 219–240 (1984).
14. A. M. Derrington, J. Krauskopf, and P. Lennie, "Chromatic mechanisms in lateral geniculate nucleus of macaque," J. Physiol. (London) **357**, 241–265 (1984).
15. R. L. De Valois and K. K. De Valois, "A multi-stage color model," Vision Res. **33**, 1053–1065 (1993).
16. C. R. Ingling, Jr., and E. Martinez, "The spatiochromatic signal of the $r-g$ channel," in *Color Vision: Physiology and Psychophysics*, J. D. Mollon and L. T. Sharpe, eds. (Academic, London, 1983), pp. 433–444.
17. F. A. A. Kingdom and K. T. Mullen, "Separating color and luminance information in the visual system," Spatial Vis. **9**, 191–219 (1995).
18. M. D'Zmura and P. Lennie, "Mechanisms of color constancy," J. Opt. Soc. Am. A **3**, 1662–1672 (1986).
19. C. Smith and J. Pokorny, "Spectral sensitivity of the foveal cone photopigments between 400 and 500 nm," Vision Res. **15**, 161–171 (1975).
20. D. Travis, *Effective Color Displays* (Academic, London, 1991), App. 4, pp. 271–272.
21. C. R. Ingling, Jr., and B. H. Tsou, "Spectral sensitivity for flicker and acuity criteria," J. Opt. Soc. Am. A **5**, 1374–1378 (1988).
22. G. Buchsbaum and A. Gottschalk, "Trichomacy, opponent color coding and optimum color information transmission in the retina," Proc. R. Soc. London, Ser. B **220**, 80–113 (1983).
23. G. Brelstaff, A. Párraga, T. Troscianko, and D. Carr, "Hyperspectral camera system: acquisition and analysis," in *Geographic Information Systems, Photogrammetry, and Geological/Geophysical Remote Sensing*, J. B. Lurie, J. J. Pearson, and E. Zillioli, eds., Proc. SPIE **2587**, 150–159 (1995).
24. J. D. Mollon, "Tho' she kneel'd in that place where they grew.... The uses and origins of primate colour vision," J. Exp. Biol. **146**, 21–38 (1989).
25. Y. Le Grand, *Form and Space Vision* (translated by Michel Millodot and Gordon G. Heat, Indiana U. Press, Bloomington and London, 1967), pp. 5–35.
26. M. V. Berry and A. N. Wilson, "Black and white fringes and the colours of caustics," Appl. Opt. **33**, 4714–4964 (1994).